

Axial Transition Form Factors and Pion Decay of Baryon Resonances

B. Juliá-Díaz* and D. O. Riska†

*Helsinki Institute of Physics and Department of Physical Sciences,
POB 64, 00014 University of Helsinki, Finland*

F. Coester‡

Physics Division, Argonne National Laboratory, Argonne, IL 60439, USA

(Dated: February 9, 2020)

Abstract

The pion decay constants of the lowest orbitally excited states of the nucleon and the $\Delta(1232)$ along with the corresponding axial transition form factors are calculated with Poincaré covariant constituent-quark models with instant, point and front forms of relativistic kinematics. The model wave functions are chosen such that the calculated electromagnetic and axial form factors of the nucleon represent the empirical values in all three forms of kinematics, when calculated with single-constituent currents. The closest description of the empirical values for the axial coupling of the nucleon and the $\Delta(1232) - N$ axial transition coupling obtains with front form kinematics. The pion decay widths calculated in instant and point form are significantly smaller than in front-form kinematics.

*Bruno.Julia@helsinki.fi

†riska@pcu.helsinki.fi

‡coester@anl.gov

I. INTRODUCTION

Quark model calculations of the pion decay widths of the baryon resonances typically fail to agree with values that have been extracted from pion-nucleon scattering data, without preference for any particular Hamiltonian model [1, 2]. This is already evident in the static quark model, in which the value for the $\pi N\Delta(1232)$ coupling leads to a $\sim 40\%$ underprediction of the decay width for the $\Delta(1232)$ resonance [3]. The likely reason for this is the restricted Hilbert space of the constituent-quark model without additional quark-antiquark configurations [4]. The problem of the pion decay widths may also reflect unrealistic features of the model wave functions and/or the associated axial quark currents. The purpose of this paper is to address this issue by a comparison of the effect of different quark currents generated by the dynamics from kinematic single-quark currents.

A relativistic constituent-quark phenomenology of baryon properties can be implemented with simple spectral representations of the mass operator. The Poincaré generators are functions of the mass and spin operators as well as kinematic quantities, which depend on the choice of a kinematic sub-group (the “form of kinematics”). Vector and axial vector currents are generated by the dynamics from single-quark currents. Single-quark current matrices are by definition functions of kinematic quark momenta and spins, which are related to internal momenta and constituent spins by boost transformations that depend on the form of kinematics.

The dependence of elastic baryon form factors of such models on the form of kinematics has been investigated in a previous paper [6]. With simple symmetric representations of the baryon states a good qualitative representation was obtained with all three forms of kinematics. Here the investigation of Ref. [6] is extended to axial transition form factors and the pion decay widths of the lowest lying resonances of the nucleon and the Δ . For the nucleon, the Δ and their positive parity excitations, $N(1440)$ and $\Delta(1600)$, the algebraic representations designed in Ref. [6] are employed. These wave functions implement the symmetries and radial shapes of hyperspherical mass operators used in [5]. The wave function of the lowest energy negative parity excitation, $N(1535)$, is constructed from the ground state wave function by imposing the short-range behavior that is implied by the centrifugal repulsion in the hyperspherical mass operator. Detailed quantitative description of the empirical features would require refinements of the baryon-states and/or the current

matrices and very likely the consideration of configurations with quark-antiquark pairs.

As the pion decay of the baryons is described by the coupling of the gradient of the pion field to the axial current of the baryons, the decay widths are proportional to the axial form factor. In the case of the higher resonances, the calculated decay widths vary significantly with the choice of kinematics. Point form kinematics yields unrealistically small values for the pion decay widths of the lowest two positive parity resonances. Front form kinematics yields values, which are commensurable with the empirically extracted imaginary parts of the resonance pole positions, even if on the average too small by $\sim 30 - 50\%$.

This paper is structured in the following way. The relevant baryon kinematics and the relations of axial currents to pion decay widths are summarized in Section 2. Section 3 contains the description of the quark representations of the baryon states and a discussion of the quark kinematics used in the construction of axial current densities. Section 4 contains a comparison of the axial transition form factors and pion decay widths that are calculated with the three different forms of kinematics. Section 6 contains a concluding discussion.

II. AXIAL TRANSITION FORM FACTORS AND PION DECAY WIDTHS

A. Baryon Kinematics

The axial transition form factors are invariant matrix elements of the axial currents. They are functions of the invariant velocity transfer,

$$\eta = \frac{1}{4}(v_f - v_a)^2, \quad (1)$$

where v_a and v_f are the 4-velocities of the initial and final baryons. The variable η is related to the invariant 4-momentum transfer as

$$Q^2 = (M_f v_f - M_a v_a)^2 = 4M_f M_a \eta - (M_f - M_a)^2. \quad (2)$$

For pionic decay, $N^* \rightarrow N + \pi$, the momentum transfer is $Q^2 = -m_\pi^2$ and

$$\eta_\pi = \frac{(M_a - M_f)^2 - m_\pi^2}{4M_f M_a}. \quad (3)$$

The covariant axial current densities $A^\mu(x)$ considered here are defined by chirally covariant Dirac spinor and Rarita-Schwinger spinor matrices,

$$\mathcal{A}_{\frac{1}{2}, \frac{1}{2}}^\mu := \gamma^\mu \gamma_5, \quad \mathcal{A}_{\frac{1}{2}, \frac{3}{2}}^{\mu\nu} := 1 g^{\mu\nu} \quad (4)$$

for $\frac{1}{2}, \frac{1}{2}$ and $\frac{1}{2}, \frac{3}{2}$ transitions. These matrices are related to the spin representations of the axial current density operator, $A^\mu(x)$, boost transformations and projections to definite intrinsic parity:

$$\langle M_f, v_f, \frac{1}{2}^+ | A_\alpha^\mu(0) | \frac{3}{2}^+, v_a, M_a \rangle = G_A^{\Delta 3/2^+}(Q^2) \bar{u}(v_f) u^\mu(v_a) \chi^\dagger \chi_\alpha, \quad (5)$$

$$\langle M_f, v_f, \frac{1}{2}^+ | A_a^\mu(0) | \frac{1}{2}^+, v_a, M_a \rangle = G_A^{N1/2^+}(Q^2) \bar{u}(v_f) \gamma^\mu \gamma_5 u(v_a) \chi^\dagger \tau_\alpha \chi, \quad (6)$$

$$\langle M_f, v_f, \frac{1}{2}^+ | A_a^\mu(0) | \frac{1}{2}^-, v_a, M_a \rangle = G_A^{N1/2^-}(Q^2) \bar{u}(v_f) \gamma^\mu u(v_a) \chi^\dagger \tau_\alpha \chi. \quad (7)$$

Here χ and χ_a denote isospin amplitudes for isospin 1/2 and 3/2 and $G_A(Q^2)$ is an invariant form factor. Explicit expressions for the spinor amplitudes $u(v)$ and $u^\mu(v)$ are listed in Appendix A.

With canonical spin the spin quantization axis is in the direction of the velocities. The choice of frame is a matter of convenience. For instance [6]:

$$v_f = \left\{ \sqrt{1+\eta}, 0, 0, \sqrt{\eta} \right\}, \quad v_a = \left\{ \sqrt{1+\eta}, 0, 0, -\sqrt{\eta} \right\}. \quad (8)$$

With this choice the canonical-spin matrices are for $(\frac{1}{2}, \frac{1}{2})$ transitions

$$\begin{aligned} \langle \frac{1}{2}^+ | A(0) | \frac{1}{2}^+ \rangle &:= G_A(Q^2) \left\{ 0, \sqrt{1+\eta} \sigma_\perp, \sigma_z \right\} \\ \langle \frac{1}{2}^+ | A(0) | \frac{1}{2}^- \rangle &:= G_A(Q^2) \left\{ 1, i\sqrt{\eta}(\hat{z} \times \vec{\sigma}), 0 \right\}, \end{aligned} \quad (9)$$

and for $(\frac{1}{2}^+, \frac{3}{2}^+)$

$$\begin{aligned} \langle \frac{1}{2}^+, \sigma' | \sqrt{\frac{1}{2}} [A_x(0) \mp i A_y(0)] | \frac{3}{2}^+, \sigma \rangle &:= -\sqrt{\frac{2}{3}} (\frac{1}{2}, 1, \sigma', \pm 1 | \frac{3}{2} \sigma) G_A(Q^2), \\ \langle \frac{1}{2}^+, \sigma' | A_z(0) | \frac{3}{2}^+, \sigma \rangle &:= -\sqrt{\frac{2}{3}} (\frac{1}{2}, 1, \sigma', 0 | \frac{3}{2} \sigma) G_A(Q^2), \quad A^0(0) = 0. \end{aligned} \quad (10)$$

Under the longitudinal Lorentz transformations,

$$\begin{aligned} v_f &= \left\{ \sqrt{1+\eta} \cosh \theta + \sqrt{\eta} \sinh \theta, 0, 0, \sqrt{\eta} \cosh \theta + \sqrt{1+\eta} \sinh \theta \right\}, \\ v_a &= \left\{ \sqrt{1+\eta} \cosh \theta - \sqrt{\eta} \sinh \theta, 0, 0, -\sqrt{\eta} \cosh \theta + \sqrt{1+\eta} \sinh \theta \right\}. \end{aligned} \quad (11)$$

the longitudinal components of the current matrices are covariant and transverse components are invariant. The Wigner rotations of the spins are the identity .

For the null-plane spin representation, with the null vector $n := \{-1, 0, 0, 1\}$, and

$$v_f := \left\{ \sqrt{1+\eta}, \sqrt{\eta}, 0, 0 \right\}, \quad v_a = \left\{ \sqrt{1+\eta}, -\sqrt{\eta}, 0, 0 \right\}, \quad (12)$$

the transverse components of the momentum transfer:

$$Q = (M_f - M_a) \frac{v_f + v_a}{2} + \frac{M_f + M_a}{2} (v_f - v_a) \quad (13)$$

are

$$Q_\perp = \sqrt{\eta} \{M_a + M_f, 0\}, \quad (14)$$

and

$$Q^2 = \frac{4M_f M_a}{(M_f + M_a)^2} Q_\perp^2 - (M_f - M_a)^2. \quad (15)$$

This is a generalization of the standard $n \cdot Q = 0$ convention to inelastic transitions where the momentum transfer may be time-like.

The null-plane spin matrices are then related to the form factors by

$$\langle \frac{1}{2}^+ | n \cdot A(0) | \frac{1}{2}^+ \rangle = \sqrt{1 + \eta} G_A(Q^2) \sigma_z, \quad \langle \frac{1}{2}^+ | n \cdot A(0) | \frac{1}{2}^- \rangle = \sqrt{1 + \eta} G_A(Q^2), \quad (16)$$

and

$$\langle \frac{1}{2}^+, \frac{1}{2} | n \cdot A(0) | \frac{3}{2}^+, \frac{1}{2} \rangle = \frac{2}{3} \left(\frac{M_f + M_a}{2\sqrt{M_a M_f}} \right) \sqrt{1 + \eta} G_A(Q^2). \quad (17)$$

B. The pion decay widths

The pion coupling to the baryons is taken to have the chiral pseudovector form:

$$\mathbb{L}(x) = -\frac{1}{2f_\pi} \partial_\mu \pi_\alpha(x) \cdot A_\alpha^\mu(x), \quad (18)$$

where f_π is the pion decay constant ($f_\pi = 93$ MeV) and A_μ is the axial current of the hadron.

The perturbation \mathcal{M}' of the mass operator is given by H' in the ‘‘rest frame’’ of the excited baryon, $\vec{p}^* = 0$. The energies of the initial baryon, the nucleon and the pion are then

$$E^* = M^*, \quad E = \sqrt{M^2 + \vec{q}^2}, \quad w := \sqrt{m_\pi^2 + \vec{q}^2}. \quad (19)$$

This implies that the perturbation \mathcal{M}' of the mass operator \mathcal{M} is represented by

$$\langle \vec{q}, \sigma_N, \tau_N, \tau_\pi | \mathcal{M}' | \mathcal{P}, I, j, \sigma, \tau \rangle := \frac{1}{\sqrt{(2\pi)^3}} \sqrt{\frac{M}{2wE}} \frac{i}{\sqrt{2f_\pi}} \langle \vec{q}, \sigma_N, \tau_N | q_\mu A_{\tau_\pi}^\mu(0) | 0, \mathcal{P}, I, j, \sigma, \tau \rangle, \quad (20)$$

where \mathcal{P} , I and j are the parity, isospin and spin of the excited baryon, and $q := \{w, -\vec{q}\}$.

As a consequence the decay width, Γ :

$$\Gamma := \frac{1}{2I+1} \sum_{\tau} \frac{1}{2j+1} \sum_{\sigma} \sum_{\sigma_N, \tau_N} \sum_{\tau_{\pi}} \times \frac{1}{2\pi} \int d^3q \delta \left(\sqrt{M^2 + q^2} + \sqrt{m_{\pi}^2 + q^2} - M^* \right) |\langle \vec{q}, \sigma_N, \tau_N, \tau_{\pi} | \mathcal{M}' | \mathcal{P}, I, j, \sigma, \tau \rangle|^2, \quad (21)$$

is proportional to $(G_A(-m_{\pi}^2)/f_{\pi})^2$. For the resonances considered here explicit expressions are [7]:

$$\Gamma_{\Delta(3/2^+)} = \frac{1}{48\pi} \left| \frac{G_A^{\Delta 3/2^+}(-m_{\pi}^2)}{f_{\pi}} \right|^2 \frac{\sqrt{q_{\pi}^2 + M^2} + M}{M^*} q_{\pi}^3, \quad (22)$$

$$\Gamma_{N(1/2^+)} = \frac{3}{16\pi} \left| \frac{G_A^{N 1/2^+}(-m_{\pi}^2)}{f_{\pi}} \right|^2 \frac{\sqrt{q_{\pi}^2 + M^2} - M}{M^*} (M^* + M)^2 q_{\pi}, \quad (23)$$

$$\Gamma_{N(1/2^-)} = \frac{1}{16\pi} \left| \frac{G_A^{N 1/2^-}(-m_{\pi}^2)}{f_{\pi}} \right|^2 \frac{\sqrt{q_{\pi}^2 + M^2} + M}{M^*} (M^* - M)^2 q_{\pi}, \quad (24)$$

where

$$q_{\pi} = \frac{\sqrt{[M^{*2} - (M - m_{\pi})^2][M^{*2} - (M + m_{\pi})^2]}}{2M^*}. \quad (25)$$

III. REPRESENTATIONS OF BARYON STATES AND QUARK KINEMATICS

A. Representations of Baryon States

The baryon states formed of 3 confined quarks and total four-momentum $P = Mv$, may be represented by functions of the form

$$\Psi_{M,j,v_a,\sigma}(\vec{v}; \vec{k}_1, \vec{k}_2, \vec{k}_3; \sigma_1, \sigma_2, \sigma_3) = \phi_{\sigma}(\vec{k}_1, \vec{k}_2, \vec{k}_3; \sigma_1, \sigma_2, \sigma_3) \delta^{(3)}(\vec{v} - \vec{v}_a). \quad (26)$$

Here \vec{k}_i and σ_i are constituent momenta and spin variables. The flavor and color variables are suppressed. The norm of the wave function ϕ_{σ} is specified by

$$\|\phi_{\sigma}\|^2 = \sum_{\sigma_1, \sigma_2, \sigma_3} \int d^3k_1 \int d^3k_2 \int d^3k_3 \delta(\vec{k}_1 + \vec{k}_2 + \vec{k}_3) \delta_{\sigma_1 + \sigma_2 + \sigma_3, \sigma} \left| \phi_{\sigma}(\vec{k}_1, \vec{k}_2, \vec{k}_3; \sigma_1, \sigma_2, \sigma_3) \right|^2, \quad (27)$$

which implies that

$$(\Psi_{M,v_f,\sigma'}, \Psi_{M,v_a,\sigma}) = \delta^{(3)}(\vec{v}_f - \vec{v}_a) \delta_{\sigma',\sigma}. \quad (28)$$

Under Poincaré transformations the velocity v transforms as a four-vector, while the total spin operator \vec{j} undergoes Wigner rotations, $\mathcal{R}_W(\Lambda, v) := B^{-1}(\Lambda v) \Lambda B(v)$ as:

$$U^{\dagger}(\Lambda, d) v U(\Lambda, d) = \Lambda v, \quad v^2 = -1, \quad U^{\dagger}(\Lambda, d) \vec{j} U(\Lambda, d) = \mathcal{R}_W(\Lambda, v) \vec{j}. \quad (29)$$

Here the boost $B(v)$ is the rotationless Lorentz transformation, which satisfies the defining relation $B(v)\{1, 0, 0, 0\} = v$.

The constituent momenta and spins undergo the same Wigner rotations:

$$U^\dagger(\Lambda) \vec{k}_i U(\Lambda) = \mathcal{R}_W(\Lambda, v) \vec{k}_i, \quad U^\dagger(\Lambda) \vec{j}_i U(\Lambda) = \mathcal{R}_W(\Lambda, v) \vec{j}_i. \quad (30)$$

The Poincaré covariance of the bound-state wave function ϕ_σ , is realized by its covariance under rotations, invariance under translations and its independence of the velocity v .

The constraint $\sum_i \vec{k}_i = 0$ is conveniently implemented by the definition of Jacobi momenta,

$$\vec{\kappa} := \sqrt{\frac{2}{3}} \left(\vec{k}_1 - \frac{\vec{k}_2 + \vec{k}_3}{2} \right), \quad \vec{q} := \sqrt{\frac{1}{2}} (\vec{k}_2 - \vec{k}_3), \quad (31)$$

which implies

$$\vec{\kappa}_1^2 + \vec{\kappa}_2^2 + \vec{\kappa}_3^2 = \vec{\kappa}^2 + \vec{q}^2. \quad (32)$$

The wave functions representing the positive parity states considered are products of the permutation symmetric spin-isospin amplitudes $\chi_{j,\sigma,\tau}$, and functions of $\mathbf{P} := \sqrt{2(\vec{\kappa}^2 + \vec{q}^2)}$, [6]

$$\phi_{n,j,\sigma,\tau}(\vec{\kappa}, \vec{q}) = \chi_{j,\sigma,\tau} \varphi_n(\mathbf{P}), \quad (33)$$

with

$$\varphi_0(\mathbf{P}) = \mathcal{N} \left(1 + \frac{\mathbf{P}^2}{4b^2} \right)^{-a}, \quad (34)$$

and

$$\varphi_1(\mathbf{P}) = \varphi_0(\mathbf{P}) \left(A(a) + B(a) \left[-\frac{12a}{(1 + \frac{\mathbf{P}^2}{4b^2})} + \frac{a(a+1)}{b^2} \frac{\mathbf{P}^2}{(1 + \frac{\mathbf{P}^2}{4b^2})^2} \right] \right). \quad (35)$$

The factor \mathcal{N} is a normalization constant and the exponent a and scale b are parameters. The constants $A(a)$ and $B(a)$ are determined, by the orthonormality condition

$$\int d^3\kappa d^3q \varphi_i(\mathbf{P}) \varphi_j(\mathbf{P}) = \delta_{ij}. \quad (36)$$

The representation of the $1/2^-$ resonance $N(1535)$ involves the permutation symmetric bilinear combination of the mixed-symmetry orbital functions $\{\vec{\kappa}, \vec{q}\}$ and the mixed-symmetry spin-isospin amplitudes $\{\chi_{\frac{1}{2}^+, \sigma, \tau}, \chi_{\frac{1}{2}^-, \sigma, \tau}\}$.

$$\phi_{\frac{1}{2}^-, \sigma, \tau}(\vec{\kappa}, \vec{q}) = \frac{1}{2} \sum_{ms} (1, \frac{1}{2}, m, s | \frac{1}{2}, s_3) \left\{ \kappa Y_{1m}(\hat{\kappa}) \chi_{\frac{1}{2}^+, \sigma, \tau} + q Y_{1m}(\hat{q}) \chi_{\frac{1}{2}^-, \sigma, \tau} \right\} \varphi_2(\mathbf{P}) \quad (37)$$

The parameters determined in Ref. [6] provide a qualitative fit to the electromagnetic form factors of the nucleon with each form of kinematics. They are listed in Table I. For the radial wave function $\varphi_2(\mathbf{P})$ the following form is employed:

$$\varphi_2(\mathbf{P}) = \frac{C\varphi_0(\mathbf{P})}{(1 + \mathbf{P}^2/4b^2)}, \quad (38)$$

where C is a normalization constant. The asymptotic behavior for large \mathbf{P} implements the short-range behavior of the Fourier transform, $\varphi(\mathbf{R})$, implied by the centrifugal repulsion [5].

B. Quark Kinematics

The kinematic quark-current matrices are functions of quark momenta that are related by kinematic boosts to the constituent momenta \vec{k}_i . With point form kinematics all Lorentz transformations are kinematic, and the velocities are kinematic variables. The canonical boost $B_c(v)$ relates the quark momentum p_i to the constituent momentum \vec{k}_i ,

$$p_i := B(v) \left\{ \sqrt{m_q^2 + \vec{k}_i^2}, \vec{k}_i \right\}. \quad (39)$$

Kinematic null-plane quark momenta p_i^+ and $p_{i\perp}$ are related to the momentum fractions ξ_i and constituent momenta $k_{i\perp}$ by

$$p_i^+ = \xi_i P^+ \quad \text{and} \quad p_{i\perp} = k_{i\perp} + \xi_i P_\perp, \quad (40)$$

and the null-plane spins are related to Dirac spinors the spinor representations of null-plane boosts [8, 9].

With instant form kinematics the boost parameters are the initial and final momenta, \vec{P}_a and \vec{P}_f . These are related kinematically only if $\vec{P}_f = -\vec{P}_a = \vec{Q}/2$. This requirement is

TABLE I: Values of the parameters of the ground state wave function used for the three different forms of kinematics. The corresponding matter radii r_0 are listed in the last column.

	m_q (MeV)	b (MeV)	a	r_0 (fm)
instant form	140	600	6	0.63
point form	350	640	9/4	0.19
front form	250	500	4	0.55

satisfied by the Lorentz transformation (11) with [6]

$$\theta := \tanh^{-1} \left[\frac{M_a - M_f}{M_f + M_a} \sqrt{\frac{\eta}{1 + \eta}} \right]. \quad (41)$$

The relation between the three momentum transfer \vec{Q} and the four-momentum transfer is then

$$\vec{Q}^2 = Q^2 - \frac{[(P_f + P_a) \cdot Q]^2}{(P_f + P_a)^2} = Q^2 + \frac{(M_f^2 - M_a^2)^2}{Q^2 + 2(M_f^2 + M_a^2)}. \quad (42)$$

The kinematic quark momenta p_i and velocities, $v_i := p_i/m_q$, are related to the constituent momenta \vec{k}_i by canonical boosts parameterized by \vec{P} ,

$$p_i := B_c(\vec{P}/M_0) \left\{ \sqrt{m_q^2 + \vec{k}_i^2}, \vec{k}_i \right\}, \quad M_0 := \sum_i \sqrt{m_q^2 + \vec{k}_i^2}. \quad (43)$$

Axial current operators are generated by the dynamics from single-quark current matrices $\bar{u}_c(p'_i)\gamma_\perp\gamma_5 u_c(p_i)$ with point and instant kinematics, and $\bar{u}_f(p'_i)\gamma^+\gamma_5 u_f(p_i)$ with null-plane kinematics.

IV. AXIAL BARYON FORM FACTORS AND PION DECAY WIDTHS

A. The axial form factor of the nucleon

The axial form factors as obtained in the three forms of kinematics and with the wave functions defined above have been given in Ref. [6]. These results are compared in Fig. 1 to the corresponding empirical values given in Ref. [10]. All the calculated form factors agree, within the uncertainty limits, with the extant data, with little dependence on the choice of kinematics, due to the fact that different spatial wave functions are employed with the different kinematic currents. The corresponding values for the axial vector coupling constant of the nucleon $G_A(0)$ are 1.1 with instant and point form kinematics, and 1.2 with front form kinematics. These values are thus smaller by 5 – 15% than the empirical value 1.267. In comparison the static quark model value 5/3 exceeds the empirical value. The front form value may be brought into agreement with the empirical value (1.26) by increasing the constituent quark mass to 285 MeV from the value 250 MeV used above. The corresponding change in the calculated axial form factor is minor, as shown by the dot-dashed line in Fig. 1.

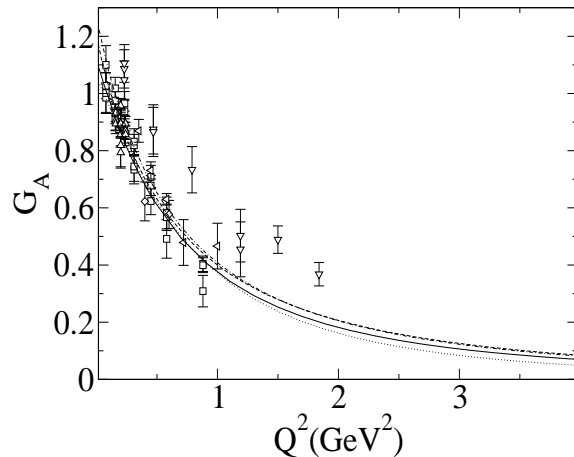


FIG. 1: Axial form factor of the nucleon. Solid, dotted and dashed lines correspond to the instant, point and front forms respectively (from [6]). The dot-dashed line corresponds to a front form calculation with a quark mass of 285 MeV.

B. The $\Delta(1232) \rightarrow N$ axial transition form factor

The calculated values for the $\Delta(1232) \rightarrow N$ transition form factor are shown in Fig. 2. The only empirical information on this form factor is that obtained by neutrino-induced reactions on the deuteron in Ref. [11]. The value for $G_A^\Delta(0)$ extracted from this experiment is $G_A^\Delta(0) = 2.4 \pm 0.25$ [3]. The present values for $G_A^\Delta(-m_\pi^2)$ that are obtained in instant and in point form kinematics are $G_A^\Delta(-m_\pi^2) = 1.75$, and $G_A^\Delta(0) = 1.72$ and thus clearly too small if still slightly larger than the quark model value 1.5 obtained in Ref. [3].

The front form calculation gives a larger value, $G_A^\Delta(-m_\pi^2) = 1.87$, which is $\sim 25\%$ below the experimental value. For comparison the static quark model value for $G_A^\Delta(-m_\pi^2)$ is $2\sqrt{2}$. It is worth noting that the experimental value for $G_A^\Delta(-m_\pi^2)$ leads to a value for the pion decay constant which is too small by 30 %.

The results obtained are consistent with the assumption of quark-antiquark components in addition to the three-quark structure of the $\Delta(1232)$, which is supported by the observation that the ratios of the experimental pionic decay widths of $\Delta \rightarrow N\pi$, $\Sigma^* \rightarrow \Sigma\pi$, and $\Xi^* \rightarrow \Xi\pi$ do not follow the simple 3-quark expectation 9 : 4 : 1 but are 12 : 4 : 1, $\Delta(1232)$ [12].

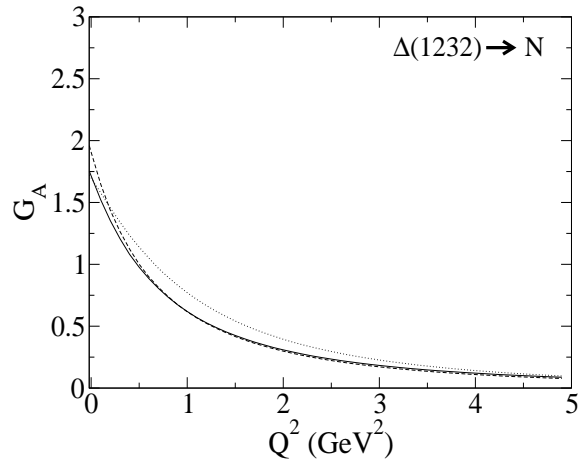


FIG. 2: Axial form factor for the $N \rightarrow \Delta(1232)$ transition. Solid, dotted and dashed lines correspond to the instant, point and front forms respectively.

C. The $N(1440) \rightarrow N$ axial transition form factor

The calculated $N(1440) \rightarrow N$ axial transition form factors are shown in Fig. 3. The shape of the form factors is similar in the three forms of relativistic kinematics. In all cases the form factors change sign near $Q^2 = 0$. With instant and point form kinematics the values at the pion point are smaller by a factor 4 than the value extracted from experiment shown in Table II. The front form value is 25% lower than the one extracted from experiment.

D. The $N(1535) \rightarrow N$ axial transition form factor

In Fig. 4 the $N(1535) \rightarrow N$ axial transition form factor is shown. The detailed evaluation is given in Appendix B. The results obtained with different kinematics are similar for this resonance, providing a value at the pion point $G_A^{N(1535)}(-m_\pi^2)$, which agrees with the value extracted from experiment, Table II.

E. The $\Delta(1600) \rightarrow N$ axial transition form factor

The axial form factors calculated with different kinematic currents are shown in Fig. 5. The differences are similar to those found for the $N(1440) \rightarrow N$ transition although the

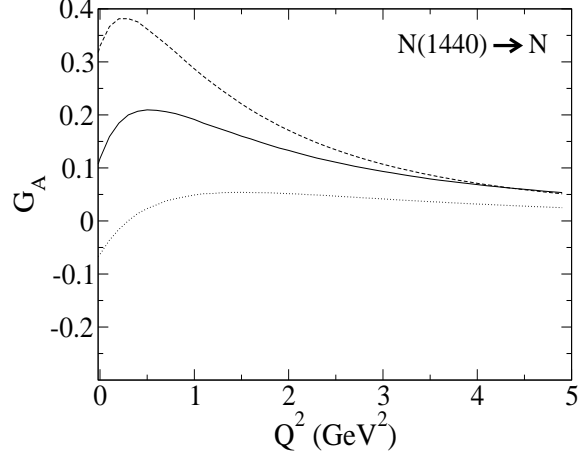


FIG. 3: Axial form factor of the $N(1440) \rightarrow N$ transition. Solid, dotted and dashed lines correspond to the instant, point and front forms respectively.

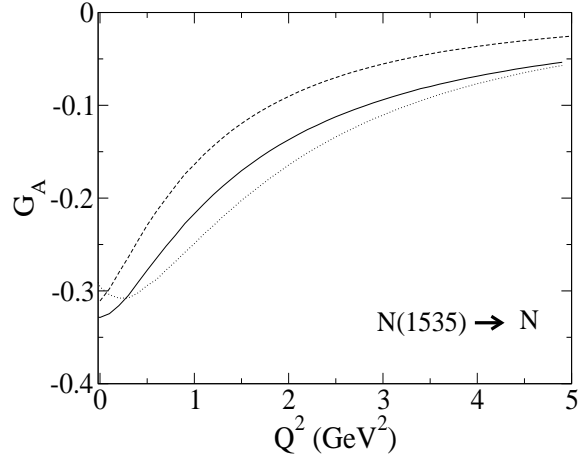


FIG. 4: Axial form factor for $N \rightarrow N(1535)$ transition. Solid, dotted and dashed lines correspond to the instant, point and front forms respectively.

difference between instant and point form are more pronounced. At the pion point front form kinematics provides a value compatible with the one extracted from experiment while point form yields an unrealistic value (Table II).

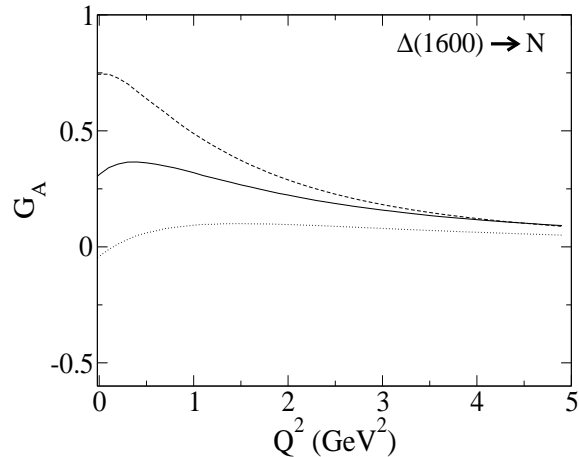


FIG. 5: Axial form factor for the nucleon to Delta(1600) transition. Solid, dotted and dashed lines correspond to the instant, point and front forms respectively.

F. Pion Decay Widths

The value of the axial form factor at the pion point, $G_A(Q^2 = -m_\pi^2)$, is related through expressions (22), (23) and (24), to the pion decay width of the corresponding resonances.

The calculated values for the pion decay widths are listed in Table III along with the empirical ranges for those values. The results in this table also reveal that only the front form results are commensurable with the empirical values, while the decay widths obtained with instant and front form kinematics are on the average too small. The failure of the point form of kinematics in providing a plausible picture of the pion decay widths has already been reported in Ref. [14].

V. DISCUSSION

The results for the calculated axial transition form factors of the baryon resonances with the present simple representations show a strong dependence on the kinematics used to generate the current operators. The spatial wave function was in each case parameterized so as to describe both the electromagnetic as well as the axial form factors of the nucleon (cf. Fig. 1). The results show a strong dependence on the representation of the excited states.

Only front form kinematics leads to a qualitatively satisfactory description of the pion decay widths. Complete agreement may require significant quark-antiquark components. Both instant and point form kinematics lead to significantly smaller values for the pion decay widths.

From the point of view of quark model phenomenology for the baryons the present results indicate a preference for front form kinematics. In comparison to the other forms of kinematics front form kinematics leads to an overall much better description of both the empirical axial vector coupling constant of the nucleon and the $\Delta(1232) - N$ axial vector transition form factor along with calculated pion decay widths that may actually agree with the corresponding empirical values.

Acknowledgments

B. J.-D. thanks the European Euridice network for support (HPRN-CT-2002-00311). Research supported in part by the Academy of Finland through grant 54038 and by the U.S. Department of Energy, Nuclear Physics Division, contract W-31-109-ENG-38.

TABLE II: Axial form factors at the pion point, $|G_A(-m_\pi^2)|$. The PHEN column contains the corresponding axial coupling constants that have been obtained phenomenologically from the imaginary parts of the corresponding resonance pole positions [13] using Eqs. (22) and (24). For front form kinematics the values (in brackets) that are obtained with the quark mass set to 285 MeV as explained in the text are also given.

	instant	point	front	PHEN
$\Delta(1232)$	1.76	1.72	1.87 [1.96]	2.67
$N(1440)$	0.11	0.07	0.29 [0.32]	[0.38–0.41]
$N(1535)$	0.33	0.29	0.31 [0.31]	[0.34–0.63]
$\Delta(1600)$	0.30	0.05	0.71 [0.74]	[0.40–0.75]

APPENDIX A: BOOSTS RELATING SPIN AND SPINOR REPRESENTATIONS

Spin and spinor representations are related by appropriate representations of the Lorentz boosts $B(v)$. For spin $\frac{1}{2}$ the spinor representation of canonical boosts $B_c(v)$ and null-plane boosts $B_f(v)$ are

$$S[B_c(v)] := D^{\frac{1}{2},0\frac{1}{2}}[B_c(v)] \oplus D^{0,\frac{1}{2}}[B_c(v)] = \frac{\vec{\alpha} \cdot \vec{v} + 1 + v^0}{\sqrt{2(1+v^0)}} \quad (\text{A1})$$

$$S[B_f(v)] := D^{\frac{1}{2},0\frac{1}{2}}[B_f(v)] \oplus D^{0,\frac{1}{2}}[B_f(v)] = \frac{\alpha_{\perp} \cdot v_{\perp} + v^+}{\sqrt{v^+}} \frac{1 + \alpha_z}{2} + \frac{1}{\sqrt{v^+}} \frac{1 - \alpha_z}{2}. \quad (\text{A2})$$

The spinor amplitudes $u_c(v)$ and $u_f(v)$ are defined by the boosts applied to the projections $(1 + \beta)/2$ onto positive intrinsic parity,

$$u_c(v) := S[B_c(v)] \frac{1 + \beta}{2}, \quad u_f(v) := S[B_f(v)] \frac{1 + \beta}{2}. \quad (\text{A3})$$

For spin 1 the appropriate boost representations are $D^{\frac{1}{2},\frac{1}{2}}[B(v)]$ and the projections are the projections onto 4-vectors with vanishing time components. It follows that the spin-1 spinor amplitudes are 4-vectors orthogonal to the velocity. With canonical boosts the result is

$$e_{\lambda}(p) := e_{\lambda} + \frac{e_{\lambda} \cdot p}{m + \omega} \left[\frac{p}{m} + n_c \right], \quad \lambda = 0 \pm 1 \quad (\text{A4})$$

with $n_c := \{1, 0, 0, 0\}$ and

$$e_{\lambda} = -\lambda \frac{\hat{e}_x + \lambda i \hat{e}_y}{\sqrt{2}} \quad \lambda = \pm 1; \quad e_0 = \hat{e}_z. \quad (\text{A5})$$

TABLE III: Pion decay widths in MeV that correspond to 2 times the imaginary pole positions in [13]. For front form kinematics the values in the brackets are obtained with a quark mass of 285 MeV as explained in the text.

	instant	point	front	PHEN [13]
$\Delta(1232)$	44	42	49 (54)	100
$N(1440)$	11	4	74 (90)	126–147
$N(1535)$	54	42	49 (49)	59–93
$\Delta(1600)$	12	0	66 (72)	30–75

With null-plane boosts the amplitudes are

$$\begin{aligned}\epsilon_\lambda(p) &:= e_\lambda - \frac{e_\lambda \cdot p}{n \cdot p} n, \quad \lambda = 0 \pm 1 \\ \epsilon_0(p) &= \frac{m}{n \cdot p} \left[n - \frac{(n \cdot p)p}{p^2} \right],\end{aligned}\tag{A6}$$

where $n := \{-1, 0, 0, 1\}$. The Rarita-Schwinger vector-spinor amplitudes of spin $\frac{3}{2}$ baryons in Eq. (5), are

$$u_\sigma^\mu(v) = \sum_{\lambda, \sigma'} \epsilon_\lambda^\mu(v) u_\sigma(v) (1, \frac{1}{2}, \lambda, \sigma' | \frac{3}{2}, \sigma).\tag{A7}$$

APPENDIX B: $N(1535) \rightarrow N$ AXIAL TRANSITION FORM FACTOR

When evaluating the transition form factor, $N(1535) \rightarrow N$, regardless of the form of kinematics, the following matrix elements need to be evaluated:

$$\langle p; \frac{1}{2} | \mathcal{X} \mathcal{F} \mathcal{S} | N(1535); \frac{1}{2} \rangle = \frac{1}{\sqrt{2}} \sum_{ms} \langle 1, \frac{1}{2}, m, s; \frac{1}{2} \frac{1}{2} \rangle \langle p, \frac{1}{2} | \mathcal{X} \mathcal{F} \mathcal{S} | N_{(1535)}^{ms} \rangle,\tag{B1}$$

where $\mathcal{X} \mathcal{F} \mathcal{S}$ is, in general, an operator that acts on spatial, flavor and spin degrees of freedom. The operator entering the actual evaluation is a Wigner or Melosh rotated axial current operator. Its flavor part is simply: $\mathcal{F} = \tau_z$. The flavor matrix elements can be evaluated leaving the spin and spatial matrix elements, which do depend on the form of kinematics. We can write the wave functions explicitly in terms of their spin, flavor (some flavor indexes have been omitted for clarity) and spatial components:

$$\begin{aligned}\langle p, \frac{1}{2} | \mathcal{X} \mathcal{F} \mathcal{S} | N_{(1535)}^{ms} \rangle &= [3]_x [3]_{FS,S}^{1/2} \mathcal{X} \mathcal{F} \mathcal{S} \frac{1}{\sqrt{2}} \left([21]_{x,S}^m [21]_{FS,S}^s + [21]_{x,A}^m [21]_{FS,A}^s \right) \\ &= \left([3]_x \mathcal{X} [21]_{x,S}^m [3]_{FS,S}^{1/2} \mathcal{F} \mathcal{S} [21]_{FS,S}^s + [3]_x \mathcal{X} [21]_{x,A}^m [3]_{FS,S}^{1/2} \mathcal{F} \mathcal{S} [21]_{FS,A}^s \right)\end{aligned}\tag{B2}$$

where the spin-flavor symmetric and mixed-symmetric wave functions are,

$$\begin{aligned}\chi_{\sigma,\tau} &\equiv [3]_{FS,S}^{\sigma,\tau} = \frac{1}{\sqrt{2}} \left([21]_{F,S}^\tau [21]_{S,S}^\sigma + [21]_{F,A}^\tau [21]_{S,A}^\sigma \right), \\ \chi_{+,\sigma,\tau} &\equiv [21]_{FS,S}^{\sigma,\tau} = \frac{1}{\sqrt{2}} \left([21]_{F,S}^\tau [21]_{S,S}^\sigma - [21]_{F,A}^\tau [21]_{S,A}^\sigma \right), \\ \chi_{-,\sigma,\tau} &\equiv [21]_{FS,A}^{\sigma,\tau} = \frac{1}{\sqrt{2}} \left([21]_{F,S}^\tau [21]_{S,A}^\sigma + [21]_{F,A}^\tau [21]_{S,S}^\sigma \right).\end{aligned}\tag{B3}$$

with the usual,

$$[3]_{S(T),S}^{l_z} = \sum_{abcm} \left(\frac{1}{2}, \frac{1}{2}, a, b | 1, m \right) \left(\frac{1}{2}, 1, c, m | \frac{3}{2}, l_z \right) \left| \frac{1}{2}, a \right| \left| \frac{1}{2}, b \right| \left| \frac{1}{2}, c \right\rangle,$$

$$\begin{aligned}
[21]_{S(T),S}^{l_z} &= \sum_{abcm} \left(\frac{1}{2}, \frac{1}{2}, a, b | 1, m\right) \left(\frac{1}{2}, 1, c, m | \frac{1}{2}, l_z\right) \left|\frac{1}{2}, a\right\rangle \left|\frac{1}{2}, b\right\rangle \left|\frac{1}{2}, c\right\rangle, \\
[21]_{S(T),A}^{l_z} &= \sum_{ab} \left(\frac{1}{2}, \frac{1}{2}, a, b | 0, 0\right) \left|\frac{1}{2}, a\right\rangle \left|\frac{1}{2}, b\right\rangle \left|\frac{1}{2}, l_z\right\rangle.
\end{aligned} \tag{B4}$$

The spin-flavor matrix elements can be split into flavor and spin parts. The only nonzero flavor matrix elements are: $[21]_{F,S} \tau_z [21]_{F,S} = -1/3$ and $[21]_{F,A} \tau_z [21]_{F,A} = 1$. Then the mixed-symmetric to symmetric part of Eq. (B3) reads:

$$\begin{aligned}
[3]_{FS,S}^{1/2} \mathcal{F} \mathcal{S} [21]_{FS,S}^s &= \frac{1}{\sqrt{2}} \left([21]_{F,S} [21]_{S,S}^{1/2} + [21]_{F,A} [21]_{S,A}^{1/2} \right) \mathcal{F} \mathcal{S} \frac{1}{\sqrt{2}} \left([21]_{F,S} [21]_{S,S}^s - [21]_{F,A} [21]_{S,A}^s \right) \\
&= \frac{1}{2} \left([21]_{F,S} \mathcal{F} [21]_{F,S} [21]_{S,S}^{1/2} \mathcal{S} [21]_{S,S}^s - [21]_{F,A} \mathcal{F} [21]_{F,A} [21]_{S,A} \mathcal{S} [21]_{S,A}^s \right) \\
&= \frac{1}{2} \left[-\frac{1}{3} [21]_{S,S}^{1/2} \mathcal{S} [21]_{S,S}^s - [21]_{S,A}^{1/2} \mathcal{S} [21]_{S,A}^s \right]
\end{aligned} \tag{B5}$$

while the mixed-antisymmetric to symmetric has the form,

$$\begin{aligned}
[3]_{FS,S}^{1/2} \mathcal{F} \mathcal{S} [21]_{FS,A}^s &= \frac{1}{\sqrt{2}} \left([21]_{F,S} [21]_{S,S}^{1/2} + [21]_{F,A} [21]_{S,A}^{1/2} \right) \mathcal{F} \mathcal{S} \frac{1}{\sqrt{2}} \left([21]_{F,S} [21]_{S,A}^s + [21]_{F,A} [21]_{S,S}^s \right) \\
&= \frac{1}{2} \left[[21]_{F,S} \mathcal{F} [21]_{F,S} [21]_{S,S}^{1/2} \mathcal{S} [21]_{S,A}^s + [21]_{F,A} \mathcal{F} [21]_{F,A} [21]_{S,A}^{1/2} \mathcal{S} [21]_{S,S}^s \right] \\
&= \frac{1}{2} \left[-\frac{1}{3} [21]_{S,S}^{1/2} \mathcal{S} [21]_{S,A}^s + [21]_{S,A}^{1/2} \mathcal{S} [21]_{S,S}^s \right].
\end{aligned} \tag{B6}$$

giving

$$\begin{aligned}
\langle p, S | \mathcal{X} \mathcal{F} \mathcal{S} | N_{(1535)}^{ms} \rangle &= \frac{1}{2\sqrt{2}} \left([3]_x \mathcal{X} [21]_{x,S}^m \left[-\frac{1}{3} [21]_{S,S}^{1/2} \mathcal{S} [21]_{S,S}^s - [21]_{S,A}^{1/2} \mathcal{S} [21]_{S,A}^s \right] \right. \\
&\quad \left. + [3]_x \mathcal{X} [21]_{x,A}^m \left[-\frac{1}{3} [21]_{S,S}^{1/2} \mathcal{S} [21]_{S,A}^s + [21]_{S,A}^{1/2} \mathcal{S} [21]_{S,S}^s \right] \right),
\end{aligned} \tag{B7}$$

and our initial matrix element reads:

$$\begin{aligned}
\langle p; \frac{1}{2} | \mathcal{X} \mathcal{Q} \mathcal{S} | N(1535), \frac{1}{2} \rangle &= \sum_{ms} \langle 1, \frac{1}{2}, m, s; \frac{1}{2} \frac{1}{2} \rangle \frac{1}{2\sqrt{2}} \\
&\quad \left([3]_x \mathcal{X} [21]_{x,S}^m \left[-\frac{1}{3} [21]_{S,S}^{1/2} \mathcal{S} [21]_{S,S}^s - [21]_{S,A}^{1/2} \mathcal{S} [21]_{S,A}^s \right] \right. \\
&\quad \left. + [3]_x \mathcal{X} [21]_{x,A}^m \left[-\frac{1}{3} [21]_{S,S}^{1/2} \mathcal{S} [21]_{S,A}^s + [21]_{S,A}^{1/2} \mathcal{S} [21]_{S,S}^s \right] \right).
\end{aligned} \tag{B8}$$

The remaining matrix elements involve integrals over the spatial wave functions, $[3]_x \mathcal{X} [21]_{x,S}^m$ and $[3]_x \mathcal{X} [21]_{x,A}^m$, together with matrix elements involving the spins, $[21]_{S,A} \mathcal{S} [21]_{S,A}^s$ and $[21]_{S,A} \mathcal{S} [21]_{S,S}^s$, which are different for the different forms of kinematics.

The spin matrix elements correspond to matrix elements of the Wigner or Melosh rotated current,

$$[21]_{S,A}^{1/2} \mathcal{S} [21]_{S,A}^s = 3 [21]_{S,A} \left[D_2^{1/2\dagger} D_2^{1/2} \right] \left[D_3^{1/2\dagger} D_3^{1/2} \right] \left[D_1^{1/2\dagger} I_{0q} D_1^{1/2} \right] [21]_{S,A}^s \tag{B9}$$

and

$$[21]_{S,A}^{1/2} \mathcal{S} [21]_{S,S}^s = 3 [21]_{S,A} \left[D_2^{1/2\dagger} D_2^{1/2} \right] \left[D_3^{1/2\dagger} D_3^{1/2} \right] \left[D_1^{1/2\dagger} I_{0q} D_1^{1/2} \right] [21]_{S,S}^s, \quad (\text{B10})$$

where $D^{1/2}$ are the representations of the corresponding Wigner or Melosh rotations for canonical and null-plane spins respectively.

-
- [1] L. Theussl *et al.*, Eur. Phys. J. A **12**, 91 (2001).
 - [2] F. Cano *et al.*, Z. Phys. A **359**, 315 (1997).
 - [3] T. Hemmert, B. R. Holstein and N. C. Mukhopadhyay, Phys. Rev. D **51**, 158 (1995).
 - [4] T. Sato and T.-S. H. Lee, Phys. Rev. C **63**, 055201 (2001); Phys. Rev. C **67**, 065201 (2003).
 - [5] F. Coester, K. Dannbom, and D.O. Riska, Nucl. Phys. A **634**, 335 (1998).
 - [6] B. Juliá-Díaz, D. O. Riska and F. Coester, Phys. Rev. C **69**, 03512 (2004).
 - [7] W. K. Cheng and C. W. Kim, Phys. Rev. **154**, 1525 (1967).
 - [8] P. L. Chung and F. Coester, Phys. Rev. D **44**, 229 (1991).
 - [9] F. Coester, Progress on Nuclear and Particle Physics, **29**, 1 (1992).
 - [10] A. Del Guerra *et al.*, Nucl. Phys. B **99**, 253 (1975); P. Brauel *et al.*, Phys. Lett. B **45**, 389 (1973); E. Amaldi *et al.*, Phys. Lett. B **41**, 216 (1972); P. Joos *et al.*, Phys. Lett. B **62**, 230 (1976); E. D. Bloom *et al.*, Phys. Rev. Lett. **30**, 1186 (1973).
 - [11] T. Kitagaki *et al.*, Phys. Rev. D **42**, 1331 (1990).
 - [12] D. O. Riska, Eur. Phys. J. A **17**, 297 (2003).
 - [13] K. Hagiwara *et al.*, Phys. Rev. C **66**, 010001 (2002).
 - [14] T. Melde, R. F. Wagenbrunn and W. Plessas, Few Body Syst. Suppl. **14**, 37 (2003).